Spectroscopically Probing Solvent-Mediated Folding in Dicarboxylate Dianions**

Torsten Wende, Marius Wanko, Ling Jiang, Gerard Meijer, Knut R. Asmis* and Angel Rubio*

Dicarboxylate salts play an important role in many areas of science including atmospheric, bio- and synthetic chemistry. For example, they are used as antitumor drugs[1], building blocks for metal-organic framework materials[2] and are found in aerosol particles comprising photochemical smog[3]. Isolated dicarboxylate dianions are stable in the gas phase and serve as model systems for multiply charged anions.[4, 5] The presence of two charge centers separated by a hydrophobic, aliphatic chain also makes them ideal for studying charge-screening and solvent-mediated effects.[6] In the present study, we use gas phase infrared (IR) spectroscopy of microhydrated suberate (SA) dianion-water clusters, $SA^{2-}(H_2O)_{0-28}$, together with quantum chemical calculations to establish relations between conformational changes and spectroscopic features. We then analyze how hydration can drive a conformational transition in a dianion and what role the hydrogen-bonded network plays.

Gas-phase action spectroscopy[7] is a powerful tool to study the effects of microhydration on the configuration of dicarboxylate dianions, adding one water molecule at a time. Anion photoelectron spectra in combination with quantum chemical calculations[6, 8, 9] found a delicate dependence of the conformation of the dicarboxylate dianion on the degree of hydration, the aliphatic chain length, as well as on temperature. A more detailed insight into the folding mechanism requires structural information, which is challenging to extract from the photoelectron data. IR photodissociation (IRPD) spectroscopy combined with high-level quantum chemical calculations on microhydrated anions[10-12] is able to supply this information and thus leads to a considerably more detailed understanding of this hydration-mediated folding process at the molecular level.

Recent IRPD spectra of SA^{2-} and its monohydrate $SA^{2-} \cdot H_2O$

[∗]   T. Wende, L. Jiang, G. Meijer, K. R. Asmis
        Fritz-Haber-Institut der Max-Planck-Gesellschaft
        Faradayweg 4-6, 14195 Berlin (Germany)
        E-mail: asmis@fhi-berlin.mpg.de

        M. Wanko, A. Rubio
        Nano-Bio Spectroscopy Group and ETSF Scientific
        Development Centre, Departamento de Física de
        Materiales, Universidad del País Vasco, Centro de Física
        de Materiales CSIC-UPV/EHU-MPC and DIPC,
        Av. Tolosa 72, E-20018 San Sebastián (Spain)
        E-mail: angel.rubio@ehu.es

revealed, how the addition of a water molecule effects the spectroscopic signature of the dianion[13]. The water molecule binds to one of the carboxylate groups of the quasi-linear dianion, causing characteristic shifts of the intense IR-active carboxylate stretching bands. In more detail, the two symmetric (ν_S) and two antisymmetric (ν_A) carboxylate stretching modes in SA^{2-} are quasi-degenerate, because each pair of modes is weakly coupled as a result of the large distance in-between the carboxylate groups. Addition of a single water molecule lifts this degeneracy and leads to a characteristic splitting of both bands (compare $n=0$ and $n=1$ spectra in Figure 1).
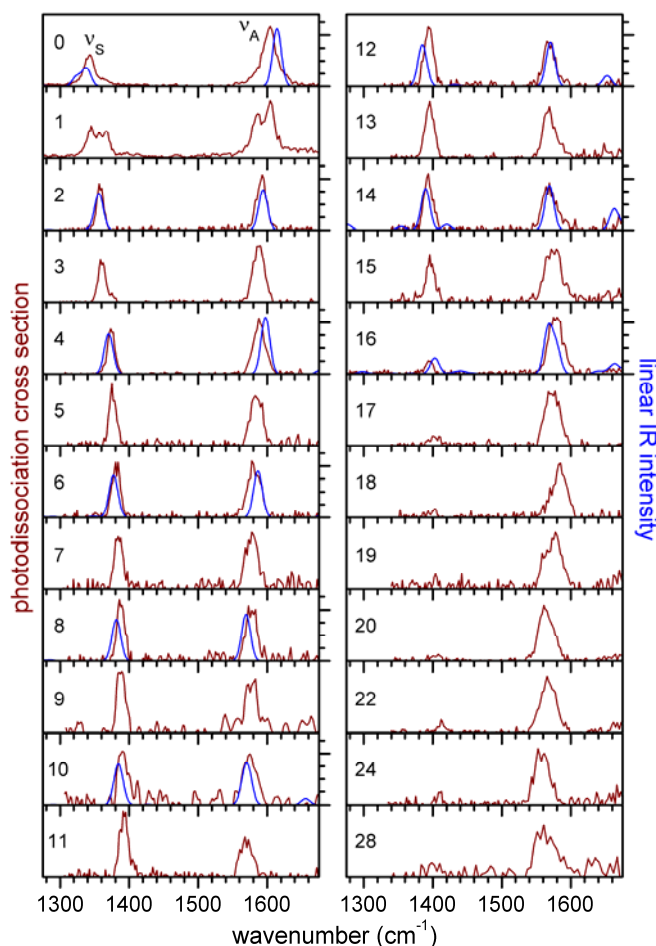

Figure 1. Experimental IRPD spectra (red) of $SA^{2-}(H_2O)_n$ clusters with $n = 0-28$ in the region of the ν_S and ν_A carboxylate stretching modes. The spectra for $n=0$ and $n=1$ are taken from Ref. [13]. Simulated linear IR absorption spectra (blue) are shown for $n=0, 2, ..., 16$.

In the present study we measured IRPD spectra of $SA^{2-}(H_2O)_n$ up to $n=28$ and these are shown in Figure 1. The ions are produced in an electrospray source at room temperature and then cooled to cryogenic temperatures by many collisions with a buffer gas prior to

irradiation with intense and tunable IR irradiation. As a probe we focus on the carboxylate stretching modes, which lie in the spectral region 1300-1650 cm^{-1}. The photodissociation cross section is plotted as a function of the photon energy. Inspection of the sequential shift of the IRPD bands as a function of the number of water molecules in the cluster (Figure 2, left) reveals that the ν_A band shifts to lower (1603 cm^{-1} → 1566 cm^{-1}) and the ν_S band (1344 cm^{-1} → 1404 cm^{-1}) shifts to higher energies with increasing number of water molecules. This sequential shift is nearly monotonic and decreases gradually with increasing n. The frequencies of aliphatic dicarboxylate dianions in bulk solution, e.g. pimelate (ν_A=1545 cm^{-1}, ν_S=1407 cm^{-1})[14] are reached for ν_S but not for ν_A (Figure 2), suggesting that the latter is more sensitive to longer range effects.
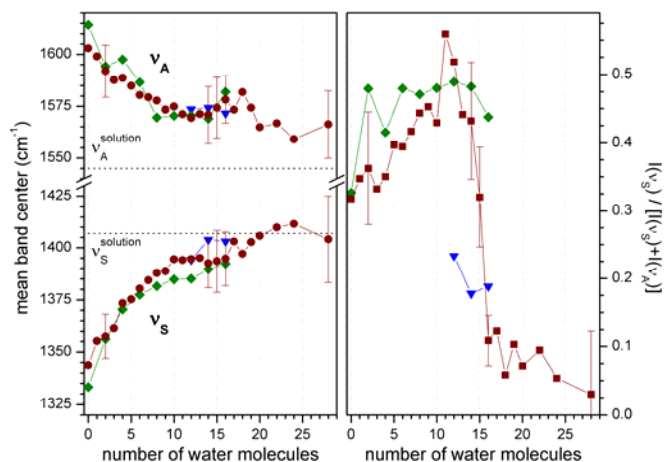

Figure 2. Center of the ν_S and ν_A bands (left) and intensity ratio I(ν_S)/[I(ν_S)+ I(ν_A)] (right) for microhydrated SA^{2-}(H$_2$O)$_n$ clusters as a function of n. Experimental values (red circles), as well as computed values for linear (green diamonds) and folded (blue triangles) geometries are shown. Error bars indicate the standard deviation (Table S1). Lines connecting the symbols are drawn to guide the eye. Doted lines indicate absorption frequencies in solution.

While the sequential band shifts are rather regular in nature, the behavior of the band intensities shows a pronounced size dependence. This is best seen in Figure 1 for the IRPD spectra of $n \geq 14$, where the intensity of the ν_S band drops significantly at n=16 and remains low throughout the spectra of the larger clusters. A more quantitative analysis, involving the normalized intensity I(ν_S)/[I(ν_S)+I(ν_a)] is plotted in Figure 2 (right). The ratio increases from 32% at n = 0 to above 50% at n=11-12, after which it drops down to 11% at n=16 and remains small for all larger water clusters.

To elucidate the origin of this behavior, we determined the minimum energy structures for both linear and folded geometries for even n up to n=16 (see Suppl. Mat.) and derived IR spectra (Figure 1, blue traces) from calculated harmonic vibrational frequencies and IR intensities. All simulated IR spectra of the folded geometries show a strong reduction in intensity of the IR-active ν_S mode, whereas the ν_A mode remains strong and decoupled, like in the linear configuration (Figure 2, right). As shown in Figure S3, this trend is independent of the particular structure of the water cluster. Note, minor deviations between the experimental IRPD cross sections and the calculated linear absorption spectra are expected, due to the multiple photon nature of the absorption process[15].

The IR intensity of a vibrational mode is proportional to the square of the change in dipole moment μ when the geometry is displaced along the corresponding normal coordinate ($|d\mu/dQ|^2$). Displacement along the ν_A mode causes a strong charge transfer

(CT) between the two carboxylate O-atoms, as it breaks the symmetry of the resonance structure. Due to the local character of this CT, it is independent of the geometry of the polyethylene chain and hence unaffected by the folding. This is in contrast to excitation of ν_S, where a smaller, but long-range, CT between the carboxylate moiety and the chain occurs, which is sensitive to changes in dihedral angles upon folding (Figure 3). Furthermore, this CT between the hydrophobic and hydrophilic moieties responds strongly to hydration and it will be affected by the mutual polarization of the carboxylates. Apart from the static polarization, we also find a subtle resonance effect due to the interaction of the fluctuating dipoles induced by excitation of ν_S (Figure 3). We isolated this effect for n=12 by calculating the spectrum with isotopically labeled oxygen on one of the two carboxylates to decouple the two resonating COO stretching modes. As a result I(ν_S) decreases in the linear and increases in folded case (Table S4).
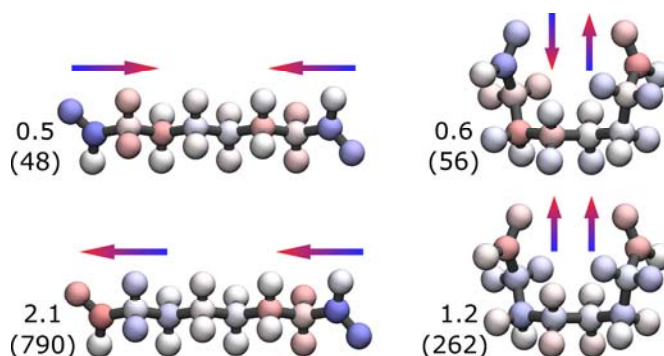

Figure 3. Natural population analysis (NPA) difference charges induced by displacement along ν_S modes for linear (left) and folded (right) n=12 clusters (water molecules not shown). |dμ/dQ| is given in 10^{-2} a.u., intensity I (in parentheses) in km/mol.

While the relation between cluster size and folding is clearly established, the investigation of the folding mechanism in the low-temperature regime remains challenging. Both experiments and classical molecular dynamics (MD) simulations face the problem that a thermodynamic equilibrium between linear and folded structures cannot be obtained at cryogenic temperatures[6, 9]. As suggested by Wang et al. [6, 9], this is due to a folding barrier that originates from the long-range Coulomb repulsion between the charged moieties, which is counteracted by additional hydrogen bonds that form in the folded structures (Table S2). Our MD simulations support this model in several respects. Even at 230 K, we find low folding/defolding rates. A typical folding event in the MD trajectory (see Suppl. Mat. for a movie for n=16) shows a three-step process. First, SA^{2-} rests in an intermediate state where the separation between the carboxylates is reduced by isomerization of two C-C bonds, i.e., the outermost C-C-C-C dihedrals assume a value of ca +/-65°. Then, the first hydrogen bond forms between the two separate water clusters, and finally, the formation of additional hydrogen bonds allows for a third C-C isomerization, which defines the folded state (Table S3).

For the n=14 complex, Wang *et al.* have shown that linear and folded structures are in an equilibrium at 108 K[6, 9]. While at higher temperatures, the linear form is more stable, a negative folding energy E_f of -1.7 kcal/mol was extrapolated for the 0-K limit. This information can be used to assess quantum chemical calculations on the minimum energy structures. To investigate the folding energetics, we performed CEPA/1 calculations (with ZPVE correction from PBE). Compared with the experimental estimate for

$n=14$, the method underestimates E_f by 4.4–4.6 (1.1–1.3) kcal/mol using a double-ζ (triple-ζ) basis set, respectively. Assuming the same error for $n=12$, the linear structure would be more stable by merely 1–2 kcal/mol at 0 K (Table 1).

Table 1: Decomposition of the folding energy E_f (kcal/mol).[a]

n	E_{Coul}[b]	SA	water	SA-water	ZPVE	E_f
12	26.5	23.0	5.6	-33.7	2.7	-2.4
14	38.7	31.1	24.0	-63.0	1.8	-6.1
16	23.2	18.6	3.5	-31.5	2.6	-6.8

[a] CEPA/1 calculations (aug-cc-pVDZ basis set and MP2/TZVP geometries); ZPVE from PBE/aug-cc-pVDZ. [b] Bare Coulomb interaction of the COO$^-$ fragments (including intermolecular CT).

A decomposition of E_f based on fragment calculations is shown in Table 1. The Coulomb repulsion between the carboxylates increases by 20–40 kcal/mol upon folding, which essentially constitutes the folding energy of the bare SA^{2-}, when omitting the water molecules in the calculation. The rise in energy is compensated by the interaction between the SA^{2-} and the water cluster and reflected in the formation of additional hydrogen bonds, mostly between the dianion and the water molecules (Table S2) Surprisingly, the water–water interaction does *not* contribute to folding, as the energy of the water cluster is not lowered by folding, when SA^{2-} is omitted in the calculation.

The present results show that (1) the intensity of the IR-active symmetric carboxylate stretching mode represents a sensitive probe to distinguish between linear and folded dicarboxylate dianions, because this mode strongly responds to the coupling between the carboxylate group and the saturated chain. (2) In contrast, the frequencies of the carboxylate stretching modes are more sensitive to the local hydrogen bonding network. Higher resolution techniques can exploit this to directly determine detailed structural information. (3) The stabilization of the folded dianion structures is essentially due to the formation of additional *solute-solvent* (rather than solvent-solvent) hydrogen bonds. Therefore, the folded structures should also persist in much larger microhdyrated clusters at sufficiently low temperature. The present findings should have important implications for probing the structure of dicarboxylic acids and their ions in the condensed phase, as well as for remote sensing applications used, e.g., in atmospheric measurements.

Experimental Section

The IRPD experiments are carried out using a ring electrode trap/time-of-flight, TOF, mass spectrometer[16, 17], temporarily installed at the "Free Electron Laser for Infrared eXperiments", FELIX, facility[18] at the FOM Institute Rijnhuizen (The Netherlands). Gas phase anions are produced in a commercial Z-spray source from a solution of suberic acid (1 mM) and NaOH (2 mM) in a 20/80 water/acetonitrile mixture. Parent ions are mass-selected in a quadrupole mass filter (Figure S1) and focused into a ring electrode ion trap. To allow for continuous ion loading and ion thermalization, the trap is continuously filled with He gas (~0.01 mbar) at an ion trap temperature of 15 K. After filling the trap for 99 ms all ions are extracted from the ion trap and focused both temporally and spatially into the center of the extraction region of an orthogonally mounted linear time-of-flight (TOF) mass spectrometer. Here, they interact with the IR laser pulse prior to the application of the extraction voltages. FELIX is operated from 1250 – 1800 cm^{-1} with a bandwidth of ~0.3% RMS of the central wavelength and average power of 30 mJ/pulse. IR spectra are recorded by monitoring all ion intensities simultaneously as the laser wavelength is scanned. The

photodissociation cross section σ is determined from the relative abundances of the parent and photofragment ions, I_0 and $I(\nu)$, and the frequency dependent laser power $P(\nu)$ using $\sigma = -\ln[I(\nu) / I_0] / P(\nu)$.[15]

MD simulations were performed with the CHARMM force field (glutamic acid parameters)[19]. For successive structure selection and optimization, the SCC-DFTB method[20], DFT (PBE/aug-cc-pVDZ) and CC2/aug-cc-pVDZ were used, the latter two as implemented in turbomole 6.1[21]. CEPA/1 (aug-cc-pVDZ basis) calculations were performed with ORCA 2.7[22]. Theoretical IR spectra show scaled (factor 1.0246) PBE/aug-cc-pVDZ frequencies. See Suppl. Mat. for computational details.

[1] M. Gielen, *Coord. Chem. Rev.* **1996**, *151*, 41-51.

[2] C. N. R. Rao, S. Natarajan, R. Vaidhyanathan, *Angew. Chem., Int. Ed.* **2004**, *43*, 1466-1496.

[3] D. Grosjean, K. Vancauwenberghe, J. P. Schmid, P. E. Kelley, J. N. Pitts, *Environ. Sci. Technol.* **1978**, *12*, 313-317.

[4] L. S. Wang, C. F. Ding, X. B. Wang, J. B. Nicholas, B. Nicholas, *Phys. Rev. Lett.* **1998**, *81*, 2667-2670.

[5] X. B. Wang, L. S. Wang, *Annu. Rev. Phys. Chem.* **2009**, *60*, 105-126.

[6] X. Yang, Y. J. Fu, X. B. Wang, P. Slavicek, M. Mucha, P. Jungwirth, L. S. Wang, *J. Am. Chem. Soc.* **2004**, *126*, 876-883.

[7] M. A. Duncan, *Int. J. Mass Spectrom.* **2000**, *200*, 545-569.

[8] B. Minofar, M. Mucha, P. Jungwirth, X. Yang, Y. J. Fu, X. B. Wang, L. S. Wang, *J. Am. Chem. Soc.* **2004**, *126*, 11691-11698.

[9] X. B. Wang, J. Yang, L. S. Wang, *J. Phys. Chem. A* **2008**, *112*, 172-175.

[10] J. M. Weber, J. A. Kelley, S. B. Nielsen, P. Ayotte, M. A. Johnson, *Science* **2000**, *287*, 2461-2463.

[11] J. Zhou, G. Santambrogio, M. Brummer, D. T. Moore, G. Meijer, D. M. Neumark, K. R. Asmis, *J. Chem. Phys.* **2006**, *125*, 111102(111101-111104).

[12] M. F. Bush, R. J. Saykally, E. R. Williams, *J. Am. Chem. Soc.* **2007**, *129*, 2220-2221.

[13] D. J. Goebbert, T. Wende, R. Bergmann, G. Meijer, K. R. Asmis, *J. Phys. Chem. A* **2009**, *113*, 5874-5880.

[14] S. E. Cabaniss, J. A. Leenheer, I. F. McVey, *Spectrochim Acta A* **1998**, *54*, 449-458.

[15] J. Oomens, A. G. G. M. Tielens, B. Sartakov, G. von Helden, G. Meijer, *Astrophys. J.* **2003**, *591*, 968-985.

[16] D. J. Goebbert, G. Meijer, K. R. Asmis, *AIP Conf. Proc.* **2009**, *1104*, 22-29.

[17] D. J. Goebbert, E. Garand, T. Wende, R. Bergmann, G. Meijer, K. R. Asmis, D. M. Neumark, *J. Phys. Chem. A* **2009**, *113*, 7584-7592.

[18] D. Oepts, A. F. G. van der Meer, P. W. van Amersfoort, *Infrared Phys. Technol.* **1995**, *36*, 297-308.

[19] A. D. MacKerell, D. Bashford, M. Bellott, R. L. Dunbrack, J. D. Evanseck, M. J. Field, S. Fischer, J. Gao, H. Guo, S. Ha, D. Joseph-McCarthy, L. Kuchnir, K. Kuczera, F. T. K. Lau, C. Mattos, S. Michnick, T. Ngo, D. T. Nguyen, B. Prodhom, W. E. Reiher Iii, B. Roux, M. Schlenkrich, J. C. Smith, R. Stote, J. Straub, M. Watanabe, J. Wiorkiewicz-Kuczera, D. Yin, M. Karplus, *J. Phys. Chem. B* **1998**, *102*, 3586-3616.

[20] M. Elstner, D. Porezag, G. Jungnickel, J. Elsner, M. Haugk, T. Frauenheim, S. Suhai, G. Seifert, *Phys. Rev. B* **1998**, *58*, 7260-7268.

[21] *TURBOMOLE V6.1 - A development of University of Karlsruhe and Forschungszentrum Karlsruhe GmbH, 1989-2007, available from http://www.turbomole.com*, TURBOMOLE GmbH, 2009.

[22] *ORCA - An Ab Initio, DFT and Semiempirical electronic structure package, Version 2.7 - Revision 0, Universität Bonn*, F. Neese, 2009.

Entry for the Table of Contents (Please choose one layout)

Layout 1: